Title

Evaluation of the disco-vertebral junction using ultrashort time-to-echo magnetic resonance imaging: inter-reader agreement and association with vertebral endplate lesions

Journal

Skeletal Radiology, 45(9)

ISSN

0364-2348

Authors

Chen, Karen C
Tran, Betty
Biswas, Reni
et al.

Publication Date

2016-09-01

DOI

10.1007/s00256-016-2413-8

Peer reviewed

HHS Public Access

Author manuscript

Skeletal Radiol. Author manuscript; available in PMC 2017 September 01.

Published in final edited form as:

Skeletal Radiol. 2016 September ; 45(9): 1249–1256. doi:10.1007/s00256-016-2413-8.

Evaluation of the Disco-Vertebral Junction Using Ultrashort Time-to-Echo Magnetic Resonance Imaging: Inter-reader Agreement and Association with Vertebral Endplate Lesions

Karen C. Chen, M.D.[1], **Betty Tran, B.S.**[1,3], **Reni Biswas, B.S.**[1,3], **Sheronda Statum, B.S., M.B.A.**[1,3], **Koichi Masuda, M.D.**[2], **Christine B. Chung, M.D.**[1,3], and **Won C. Bae, Ph.D.**[1,3]

[1]Radiology Service, VA San Diego Healthcare System, 3350 La Jolla Village Drive, MC 114, San Diego, CA 92161

[2]Department of Orthopaedic Surgery, University of California, San Diego, 9500 Gilman Drive, MC 0863, San Diego, CA 92093-0863

[3]Department of Radiology, University of California, San Diego, 9427 Health Sciences Drive, San Diego, CA 92093-0997

Abstract

Objective—To evaluate ultrashort time to echo (UTE) magnetic resonance (MR) morphology of the cartilaginous endplates (CEP) in cadaveric lumbar spines with bony vertebral endplate (VEP) lesions, to determine inter-reader agreement as well as associations between the CEP morphology and VEP lesions as well as other abnormalities.

Materials and Methods—MR imaging of cadaveric lumbar spines from 10 donors was performed at 3T using a UTE MR sequence. Two musculoskeletal radiologists identified the location of vertebral endplate lesions in consensus. The morphology of the CEP overlying the lesions and in the adjacent normal regions was assessed individually. A total of 55 vertebral lesions and 55 normal regions were assessed. The presence of osteophytosis, morphological changes of the anterior and posterior longitudinal ligament, and intervertebral disc signal and morphology was also assessed. Agreement between observers was determined using Cohen's kappa analysis, and association between CEP and vertebral endplate lesions was determined using chi square test.

Results—55 vertebral endplate lesions were identified and the morphology of CEP evaluated by two readers was in substantial agreement with Cohen's kappa of 0.78. The presence of vertebral endplate abnormality was associated with the presence of osteophytes (39 out of 55 levels), altered morphology and signal of the anterior longitudinal ligament (23 out of 55 levels) and intervertebral discs (30 out of 55 levels).

Conclusion—UTE MRI enables evaluation of the CEP with substantial inter-reader agreement. Abnormal changes of the CEP may facilitate formation of lesions of vertebral endplate over time and are associated with degenerative changes of the lumbar spine.

[3]Corresponding Author: Won C. Bae, Ph.D., TEL: (858) 822-1204, FAX: (858) 822-1331, wbae@ucsd.edu.

Disclosure: The authors declare that they have no conflict of interest

Keywords

Schmorl's node; disc degeneration; lumbar spine; osteophyte; back pain

INTRODUCTION

Chronic low back pain is a common problem and is the second most common cause of disability in US adults, accounting for 17% of all patients with disabilities, and resulting in lost workdays (1,2). Chronic low back pain can be challenging to diagnose and treat. The etiology for back pain may arise from sensitized nociceptors in the annulus fibrosus of degenerated discs (annulogenic pain) or at the richly innervated vertebral endplate (vertebrogenic pain) (3,4). Therefore, differentiating between these pain generators may help determine the choice of therapy, those focused on altering cell function versus biological implants.

The anatomical regions of the intervertebral disc include the central nucleus pulposus, the peripheral fibrocartilaginous annulus fibrosus, and the superior and inferior cartilaginous endplates (CEP). The CEP is a thin layer of hyaline cartilage located between the avascular intervertebral disc and the bony vertebral endplate. It plays an important role in the function and homeostasis of the disc by serving as a mechanical stabilizer as well as a pathway for nutrient transport (5). Vascular canals, found in calcified portions of the CEP, help supply nutrients to the disc (6). Structural and compositional age-related changes occur in the CEP and include thinning of the CEP and calcification of the cartilage, which may inhibit the passage of nutrients to the disc and lead to subsequent disc degeneration (7). Bony vertebral endplates (VEP) also undergo changes with aging and injury. Various forms of endplate lesions including Schmorl nodes, fractures, avulsions/erosions, and calcifications have been described. Schmorl nodes are focal indentations of the VEP containing herniated nucleus pulposus (8-11), with an unclear etiology. Congenital Schmorl nodes, arising from cartilage defects created after notochord regression, may be asymptomatic, while traumatic or degenerative Schmorl nodes from failure of the VEP, are more likely to be symptomatic (12). Peng et al. suggested that Schmorl nodes may share an pathoetiology with osteonecrosis with fibrosis within the marrow cavities beneath the CEP and the disappearance of adipocytes and osteocytes (13). Schmorl nodes are found with ~10% frequency in MR examination of normal subjects, but with a significantly higher (~20%) frequency in those with back pain (14). Stäbler et al. showed that vascularized Schmorl nodes with adjacent degenerative bone marrow edema were more likely to be larger and correlate with back pain (15). In a post-mortem study, endplate lesions of Schmorl node and calcification were found to be significantly associated with a history of back pain (16). Bony endplate innervation may also be increased in areas of bone damage, likely accounting for clinical symptoms of back pain (17). While of unclear etiology, it is speculated that VEP lesions may be related to structural or biomechanical changes of the adjacent CEP. These may include focal thinning (18) and/or biomechanical weakening (19) of the CEP, which may lead to focal vulnerability of the VEP. These changes, alone or in combination with weakening or a loss of bone mineral density of the VEP (20), may result in a VEP lesion.

The relationship between CEP and VEP is not known, due in part to the lack of suitable imaging technique to evaluate the CEP in the past. While VEP changes can be non-invasively imaged using a number of methods, including radiography (8,10), computed tomography (21), and conventional MRI (11), the CEP is not evaluated routinely using these imaging modalities. In the past, T1-weighted (T1W) and T2-weighted (T2W) MRI has been used to identify the vertebral endplate and characterize endplate defects and associated marrow changes (15,22). Standard clinical MR sequences, with minimum TE of 10 ms or greater, target the longer T2 structures of the spine, specifically the nucleus pulposus, which has a T2 value of ~100 msec. With conventional MR sequences, bony VEP (with T2 value of less than 1 ms (23)) is hypointense and there is inadequate contrast to separate it from the CEP, which is also hypointense due to its intrinsically short T2 property of approximately 3 ms (24). Therefore, despite the availability of a variety of magnetic resonance (MR) imaging sequences, the CEP is only directly imaged by relatively few sequences including ultrashort time-to-echo (UTE) (**Figure 1abc**), as shown in our recent study comparing histology of CEP samples with UTE and conventional MRI sequences (25).

A non-invasive and sensitive method of detecting CEP changes would be of considerable value for evaluation of early pathologic changes of the disco-vertebral junction. Objective of this study was to evaluate UTE MR morphology of the CEP in cadaveric lumbar spines with VEP lesions, to determine inter-reader agreement in CEP evaluation. In addition, associations between the CEP morphology and VEP lesions as well as other abnormalities of the lumbar spines were determined.

MATERIALS AND METHODS

This article does not contain any studies with human participants or animals performed by any of the authors. This cadaveric study was exempt by the institutional review board and the consent was not required. This article does not contain identifiable patient data.

Samples

Cadaveric lumbar spines containing T12 to S1 were obtained from 10 donors (9 male, 1 female; mean age 56.2 years, standard deviation 8.2 years) within 2 days of death for MR imaging. Samples were imaged within a few hours of resection, and were not stored frozen.

MR Imaging

MR imaging was performed with a 3 Tesla General Electric Signa HDx scanner (GE Healthcare, Milwaukee, MI) with clinical 8-channel knee coil. The MR scanner had the maximum peak gradient amplitude of 40 mT/m and slew rate of 150 mT/m/s. Hardware modification included the addition of a custom transmit-receive switch to the receiver pre-amplifiers for rapid switching after the radiofrequency excitation pulse to achieve the minimum echo time of 8 microseconds. Each specimen was placed in the scanner in the head-first and prone position, and imaged in the sagittal plane in a multi-slice setting (5 slices). Imaging protocol included UTE morphologic sequence tailored for short T2 tissues of the disco-vertebral junction, and conventional Multi-Echo Spin Echo T2 (ME SE T2) mapping quantitative sequence tailored for long T2 components of the disc. **Table 1** lists

detailed scanning parameters used with each sequence. UTE echo subtraction images were created (**Figure 1c**) by digitally subtracting 2nd echo image (**Figure 1b**) from the 1st echo image (**Figure 1a**), without rescaling.

MR Evaluation

On the UTE echo subtraction images, VEP lesions were identified in consensus by two musculoskeletal radiologists with 17 and 4 years of experience. Vertebral endplate lesions included Schmorl's nodes, and other irregularity in VEP contour in MR images. While these VEP lesion types were observed and devised at the time of the study, majority have been described previously in the literature. Schmorl's nodes were defined as localized vertebral endplate irregularities containing herniation of intervertebral disc (8-11,26,27). There were “classic” Schmorl nodes with abrupt and focal indentation of the VEP (**Figure 2a**, box), as well as those with more smooth indentation (**Figure 3a**, box). Other irregularities included fractures (discontinuous disruption (10,11); **Figure 4a**, box) and other focal deviations of the VEP contour from the norm (11). There were no samples with MR images suggesting a developmental or metabolic diseases such as Scheuermann's disease with multiple VEP lesions on superior and inferior surfaces (28,29) or hyperparathyroidism with obvious subchondral resorption of vertebrae (29) beneath the VEP lesion. A total of 27 images out of 50 slices were identified with one or more VEP lesions and these slices underwent further evaluation.

On these images, each reader individually evaluated the morphology of the CEP overlying the lesion (**Figure 2a**, box), and the CEP in the adjacent normal region (**Figure 2a**, dotted box). In total, 55 VEP lesions and 55 adjacent normal regions were evaluated. Following classifications of CEP morphology were found: normal CEP morphology consisted of continuous linear high signal intensity (**Figure 1c**, arrows), while marked thinning (**Figure 2a**, arrowheads), absent cartilaginous endplates (**Figure 3a**, arrowhead), diffuse thickening (**Figure 4a**, arrowhead) or any other irregularity of the high signal intensity of the CEP was considered abnormal.

In other regions of the lumbar spine, degenerative morphologic changes, including the presence of osteophytes (**Figure 4a**, curved arrow), thickening of the anterior or posterior longitudinal ligaments (**Figure 2a**, curved arrow), and abnormal signal and morphology of the intervertebral disc (**Figure 5**) were also evaluated by one of the readers who assessed endplate morphology.

Statistical Analysis

The agreement of CEP morphology between two readers was determined using Cohen's kappa analysis (30). The associations between VEP lesions and CEP pathology, osteophytes, thickening of longitudinal ligaments, and disc degeneration, were determined using chi square tests (31).

RESULTS

Statistics on VEP Lesions

There were a total of 55 VEP lesions found. These included 16 classic Schmorl nodes, 10 smooth indentation of the VEP, and 29 other irregular VEP lesions. In general, there was greater number of VEP lesions (any type) found at higher levels (i.e., T12 to L3) than lower levels (i.e., L3 to L5) of the spine (**Table 2**), similar to the distribution of Schmorl nodes described in past studies (19,32).

Inter-Reader Agreement on CEP morphology

Morphology of CEP evaluated by two readers was in substantial agreement with Cohen's kappa of 0.78. In all, 98 out of 110 observations (89%) were in agreement, including 44 of 55 observations over normal VEPs and 54 of 55 observations over the VEP lesions. This suggested a high sensitivity (98%) and a moderate specificity (80%) towards detecting abnormal CEP morphologies. Disagreements most often occurred while evaluating CEPs over normal regions adjacent to Schmorl nodes (7 of 11).

Association of CEP morphology with VEP lesions

Cartilage endplate abnormality was significantly ($p<0.001$) associated with VEP lesions. CEPs overlying normal VEPs were generally normal (43 out of 44 in consensus), while those overlying VEP lesions were abnormal (54 out of 54 in consensus). Amongst abnormal CEPs overlying VEP lesions, irregular (23 of 54) and thin (19 of 54) morphologies were the most frequent findings, while thickening (7 of 54) and total absence (5 of 54) of the linear signal intensity were less frequently found (**Table 3**). Amongst different types of VEP lesions (classic Schmorl nodes, smooth, irregular), the distribution of various CEP pathologies was similar (**Table 3**). A lone exception was a high prevalence of irregular CEP being found over irregular VEP lesions (17 of 29).

In addition, osteophytes (39 of 55), thickened anterior longitudinal ligaments (23 of 55), and abnormal disc signal or morphology (30 of 55) were found frequently at the levels with VEP lesions. Compared with the normal CEP/VEP levels (**Figure 5a**), in the presence of CEP and VEP abnormalities, the annulus fibrosus (**Figure 5b**, diagonal arrow) demonstrated decreased signal intensity and disorganization of the normally striated pattern (**Figure 5a**, diagonal arrow). At the abnormal levels, the anterior longitudinal ligament (**Figure 5b**, up arrow) was demonstrated with increased thickness, inhomogeneous hyperintense signal alteration and buckling of the ligamentous fibers compared to the smooth, linear, undulating pattern (**Figure 5a**, up arrow) at normal CEP/VEP levels.

DISCUSSION

This study investigated the relationship between VEP lesions and UTE MR morphology of the overlying CEP as well as other structures of the lumbar spine. We first established a substantial inter-reader reliability of morphological assessments of the CEP, with a high sensitivity and moderate specificity for detecting abnormal morphology of the CEP. Consensus interpretation by two experienced readers showed a strong association between

VEP lesions and abnormal CEP morphology, evident by the fact that all of the CEPs overlying the VEP lesions had some type of abnormal morphology. In addition, there were significant associations between VEP lesion and other degenerative changes of the spine including osteophytosis, intervertebral disc abnormality and thickening of the longitudinal ligaments.

The association between abnormal CEP morphology with VEP lesions suggests a possible role of the CEP in the development of VEP lesions. While the sequelae of events leading to a VEP lesion or CEP abnormality is not yet clear, studies have suggested a significant biomechanical role of the CEP in the integrity of the disco-vertebral junction to withstand axial loading. In a finite element model (33) with and without cartilage endplate, it was shown that the lack of cartilage endplate significantly raised Von Mises stress (related to mechanical failure) at the attachment area of the annulus fibrosus to the VEP as well as the VEP itself when the models simulated a set of spinal motions. In addition, congenitally weak area of CEP may exist adjacent to the nucleus pulposus (29), resulting in often centrally-located (16) classic Schmorl nodes. While these studies suggest protective role of a normal, functioning CEP, it remains uncertain whether the CEP or the VEP is the tissue of initial failure. Longitudinal studies to evaluate the time course of changes in both the CEP and the VEP would clarify this further.

A number of different UTE MR morphologies of the CEP were found over VEP lesions. Abnormal thinning and absence of the signal intensity maybe related to progressive resorption of the articular cartilage with replacement by subchondral bone (18) which would result in thinning and disappearance of the CEP, as has been noted in histology of aging human spines (18). There is also some evidence that dense calcifications is another possibility for irregularity or absence (34), as dense calcium deposits would yield very little signal even on UTE MR images and lead to focal absence or irregularity of the signal intensity, depending on the severity of calcification. Diffuse thickening of the cartilaginous endplate was a puzzling finding over some of the vertebral endplate defects. This change in morphology may be similar to the hypertrophy of the articular cartilage in early knee osteoarthrosis (35,36) where vascular ingrowth results in hypertrophied chondrocytes and a thickened layer of hyaline cartilage.

A substantial agreement between the readers when evaluating the CEP morphology suggests usefulness of UTE MR evaluation of the disco-vertebral junction. Overall, UTE MR evaluation of the disco-vertebral junction shows a high sensitivity (99%) and moderate specificity (80%). Disagreement in interpretation of the morphology of the CEP between readers of the CEP was most notable in areas adjacent to Schmorl nodes. This may be due to the gradual thinning of the CEP near the rim of Schmorl nodes, leading to a disagreement about its morphology.

Our study found association between VEP abnormalities and traditional MR findings of degenerative spine disease including, osteophyte formation and morphological changes in the intervertebral disc and longitudinal ligaments. The finding suggests possible remodeling of vertebral bodies and adjacent soft tissues as lumbar spine degenerates. As in the knee, adaptations to abnormal stresses in the disco-vertebral complex are not confined to the

connective tissue, but may affect the joint structures as a whole. Degenerative changes of the intervertebral discs are well established on T2-weighted MR images according to the Pfirrmann classification (37). In this classification, the normal disc (Grade 1) demonstrates bright hyperintense signal and normal disc height while inhomogeneity of the intervertebral disc signal and progressive loss of the distinction between the annulus fibrosus and nucleus pulposus characterizes progressive degenerative disc disease. Ultimately, heterogeneous hypointense disc signal and loss of the disc space is seen in end-stage degeneration (Grade 5). However, the morphologic changes of the intervertebral disc and the adjacent longitudinal ligaments on UTE MRI have not been assessed previously. Given short T2 values of the annulus fibrosus and longitudinal ligaments, these structures are normally hypointense on conventional T2-weighted sequences. However, our study shows that signal changes within these tissues can be unmasked with UTE sequences, revealing additional morphology not seen with conventional MRI.

Our study is limited by a relatively small sample size and inability to correlate radiologic findings with patient symptoms or histologic references. Unfortunately, the spines imaged in this study were further dissected for another study and histologic comparison could not be made. Another limitation is that we had a larger number of male than female donors, potentially affecting our study's ability to be generalized into a population where back pain and disc degeneration is more common in women than men.

Future directions include assessment of histopathology, as well as biomechanical properties of the disco-vertebral junction at areas with and without UTE MR abnormalities of the CEP. Quantitative UTE MRI is also possible, but may be challenging in vivo due to the trade-off between long scan time and low spatial resolution. Our preliminary work (38) and others (39,40) have shown in vivo feasibility of spines evaluation using UTE MRI. Application of UTE MRI to asymptomatic and symptomatic subjects will help to better understand the natural progression of changes, as well as roles of, the CEP and the VEP. Lastly, as the primary pathway for nutrient support, changes in the CEP may influence the diffusion of nutrients into and out of the intervertebral discs, and thus transport function of normal and abnormal CEPs would be useful to evaluate as well.

In conclusion, UTE MRI detects several types of abnormalities in the CEP signal intensity, with high sensitivity and inter-reader agreement. In addition, this study suggests significant association between CEP abnormality and VEP lesions. Additional studies to determine sequelae of changes in the CEP and VEP in a wider range of ages, as well as comparison of MR pathology to reference measures of tissue structure and function, may provide insight into the pathoetiology of VEP lesions.

ACKNOWLEDGMENT

Authors would like to thank Todd Griffith (LifeSharing, San Diego, CA) and Scott Barton (University of California, San Diego, Anatomic Services) for their assistance with cadaveric specimens.

GRANT SUPPORT

This article was made possible in part by grants from the National Institute of Arthritis and Musculoskeletal and Skin Diseases of the National Institutes of Health in support of Dr. Won C. Bae (Grant Number R01 AR066622), and Award Number 5I01CX000625 (Project ID: 1161961) from the Clinical Science Research & Development of

the VA Office of Research and Development in support of Dr. Christine B. Chung. The contents of this paper are solely the responsibility of the authors and do not necessarily represent the official views of the National Institutes of Health or Veterans Affairs.

REFERENCES

1. Freburger JK, Holmes GM, Agans RP, et al. The rising prevalence of chronic low back pain. Arch Intern Med. 2009; 169(3):251–258. [PubMed: 19204216]
2. Stewart WF, Ricci JA, Chee E, Morganstein D, Lipton R. Lost productive time and cost due to common pain conditions in the US workforce. JAMA. 2003; 290(18):2443–2454. [PubMed: 14612481]
3. van Dieen JH, Weinans H, Toussaint HM. Fractures of the lumbar vertebral endplate in the etiology of low back pain: a hypothesis on the causative role of spinal compression in aspecific low back pain. Med Hypotheses. 1999; 53(3):246–252. [PubMed: 10580532]
4. Fagan A, Moore R, Vernon Roberts B, Blumbergs P, Fraser R. ISSLS prize winner: The innervation of the intervertebral disc: a quantitative analysis. Spine (Phila Pa 1976). 2003; 28(23):2570–2576. [PubMed: 14652473]
5. Moore RJ. The vertebral end-plate: what do we know? Eur Spine J. 2000; 9(2):92–96. [PubMed: 10823423]
6. Crock HV, Goldwasser M. Anatomic studies of the circulation in the region of the vertebral end-plate in adult Greyhound dogs. Spine (Phila Pa 1976). 1984; 9(7):702–706. [PubMed: 6505840]
7. Lee SW, Mathie AG, Jackson JE, Hughes SP. Investigation of vertebral “end plate sclerosis”. Skeletal Radiol. 2001; 30(8):454–459. [PubMed: 11479751]
8. Chan KK, Sartoris DJ, Haghighi P, et al. Cupid's bow contour of the vertebral body: evaluation of pathogenesis with bone densitometry and imaging-histopathologic correlation. Radiology. 1997; 202(1):253–256. [PubMed: 8988219]
9. Solgaard Sorensen J, Kjaer P, Jensen ST, Andersen P. Low-field magnetic resonance imaging of the lumbar spine: reliability of qualitative evaluation of disc and muscle parameters. Acta Radiol. 2006; 47(9):947–953. [PubMed: 17077047]
10. Pfirrmann CW, Resnick D. Schmorl nodes of the thoracic and lumbar spine: radiographic-pathologic study of prevalence, characterization, and correlation with degenerative changes of 1,650 spinal levels in 100 cadavers. Radiology. 2001; 219(2):368–374. [PubMed: 11323459]
11. Jensen TS, Sorensen JS, Kjaer P. Intra- and interobserver reproducibility of vertebral endplate signal (modic) changes in the lumbar spine: the Nordic Modic Consensus Group classification. Acta Radiol. 2007; 48(7):748–754. [PubMed: 17729006]
12. Abu-Ghanem S, Ohana N, Abu-Ghanem Y, Kittani M, Shelef I. Acute schmorl node in dorsal spine: an unusual cause of a sudden onset of severe back pain in a young female. Asian Spine J. 2013; 7(2):131–135. [PubMed: 23741552]
13. Peng B, Wu W, Hou S, Shang W, Wang X, Yang Y. The pathogenesis of Schmorl's nodes. J Bone Joint Surg Br. 2003; 85(6):879–882. [PubMed: 12931811]
14. Hamanishi C, Kawabata T, Yosii T, Tanaka S. Schmorl's nodes on magnetic resonance imaging. Their incidence and clinical relevance. Spine (Phila Pa 1976). 1994; 19(4):450–453. [PubMed: 8178234]
15. Stabler A, Bellan M, Weiss M, Gartner C, Brossmann J, Reiser MF. MR imaging of enhancing intraosseous disk herniation (Schmorl's nodes). AJR Am J Roentgenol. 1997; 168(4):933–938. [PubMed: 9124143]
16. Wang Y, Videman T, Battie MC. ISSLS prize winner: Lumbar vertebral endplate lesions: associations with disc degeneration and back pain history. Spine (Phila Pa 1976). 2012; 37(17): 1490–1496. [PubMed: 22648031]
17. Antonacci MD, Mody DR, Rutz K, Weilbaecher D, Heggeness MH. A histologic study of fractured human vertebral bodies. J Spinal Disord Tech. 2002; 15(2):118–126. [PubMed: 11927820]
18. Bernick S, Cailliet R. Vertebral end-plate changes with aging of human vertebrae. Spine (Phila Pa 1976). 1982; 7(2):97–102. [PubMed: 7089697]

19. Begg AC. Nuclear herniations of the intervertebral disc; their radiological manifestations and significance. J Bone Joint Surg Br. 1954; 36-B(2):180–193. [PubMed: 13163100]
20. Hansson T, Roos B. The amount of bone mineral and Schmorl's nodes in lumbar vertebrae. Spine (Phila Pa 1976). 1983; 8(3):266–271. [PubMed: 6623194]
21. Silva MJ, Wang C, Keaveny TM, Hayes WC. Direct and computed tomography thickness measurements of the human, lumbar vertebral shell and endplate. Bone. 1994; 15(4):409–414. [PubMed: 7917579]
22. Chung CB, Vande Berg BC, Tavernier T, et al. End plate marrow changes in the asymptomatic lumbosacral spine: frequency, distribution and correlation with age and degenerative changes. Skeletal Radiol. 2004; 33(7):399–404. [PubMed: 15138721]
23. Du J, Bydder GM. Qualitative and quantitative ultrashort-TE MRI of cortical bone. NMR in biomedicine. 2013; 26(5):489–506. [PubMed: 23280581]
24. Bae WC, Biswas R, Chen K, Chang EY, Chung CB. UTE MRI of the Osteochondral Junction. Current radiology reports. 2014; 2(2):35. [PubMed: 25061547]
25. Bae WC, Statum S, Zhang Z, et al. Morphology of the cartilaginous endplates in human intervertebral disks with ultrashort echo time MR imaging. Radiology. 2013; 266(2):564–574. [PubMed: 23192776]
26. Fardon DF, Williams AL, Dohring EJ, Murtagh FR, Gabriel Rothman SL, Sze GK. Lumbar disc nomenclature: version 2.0: Recommendations of the combined task forces of the North American Spine Society, the American Society of Spine Radiology and the American Society of Neuroradiology. Spine J. 2014; 14(11):2525–2545. [PubMed: 24768732]
27. Fardon DF, Milette PC. Nomenclature and classification of lumbar disc pathology. Recommendations of the Combined task Forces of the North American Spine Society, American Society of Spine Radiology, and American Society of Neuroradiology. Spine (Phila Pa 1976). 2001; 26(5):E93–E113. [PubMed: 11242399]
28. Paajanen H, Alanen A, Erkintalo M, Salminen JJ, Katevuo K. Disc degeneration in Scheuermann disease. Skeletal Radiol. 1989; 18(7):523–526. [PubMed: 2588031]
29. Resnick D, Niwayama G. Intravertebral disk herniations: cartilaginous (Schmorl's) nodes. Radiology. 1978; 126(1):57–65. [PubMed: 339268]
30. Cohen J. A coefficient of agreement for nominal scales. Educational and psychological measurement. 1960
31. Yates F. Contingency Tables Involving Small Numbers and the χ² Test. Supplement to the Journal of the Royal Statistical Society. 1934; 1:217–235.
32. Hilton RC, Ball J, Benn RT. Vertebral end-plate lesions (Schmorl's nodes) in the dorsolumbar spine. Ann Rheum Dis. 1976; 35(2):127–132. [PubMed: 942268]
33. Noailly J, Lacroix D, Planell JA. Finite element study of a novel intervertebral disc substitute. Spine (Phila Pa 1976). 2005; 30(20):2257–2264. [PubMed: 16227887]
34. Bae WC, Xu K, Inoue N, Bydder GM, Chung CB, Masuda K. Ultrashort time-to-echo MRI of human intervertebral disc endplate: association with endplate calcification. Proc Int'l Soc Magn Reson Med. 2010; 18:3218.
35. Calvo E, Palacios I, Delgado E, et al. Histopathological correlation of cartilage swelling detected by magnetic resonance imaging in early experimental osteoarthritis. Osteoarthritis Cartilage. 2004; 12(11):878–886. [PubMed: 15501403]
36. Le Graverand MP, Buck RJ, Wyman BT, et al. Change in regional cartilage morphology and joint space width in osteoarthritis participants versus healthy controls: a multicentre study using 3.0 Tesla MRI and Lyon-Schuss radiography. Ann Rheum Dis. 2010; 69(1):155–162. [PubMed: 19103634]
37. Pfirrmann CW, Metzdorf A, Zanetti M, Hodler J, Boos N. Magnetic resonance classification of lumbar intervertebral disc degeneration. Spine (Phila Pa 1976). 2001; 26(17):1873–1878. [PubMed: 11568697]
38. Bae WC, Karunanithi PS, Znamirowski R, Statum S, Du J, Chung CB. Ultrashort Time-to-Echo MRI of Cartilaginous Endplates of Human Lumbar Spines In Vivo: a Feasibility Study. Radiol Soc North Am. 2013; 99:SSQ13–05.

39. Hall-Craggs MA, Porter J, Gatehouse PD, Bydder GM. Ultrashort echo time (UTE) MRI of the spine in thalassaemia. Br J Radiol. 2004; 77(914):104–110. [PubMed: 15010381]

40. Law T, Anthony MP, Chan Q, et al. Ultrashort time-to-echo MRI of the cartilaginous endplate: technique and association with intervertebral disc degeneration. J Med Imaging Radiat Oncol. 2013; 57(4):427–434. [PubMed: 23870338]

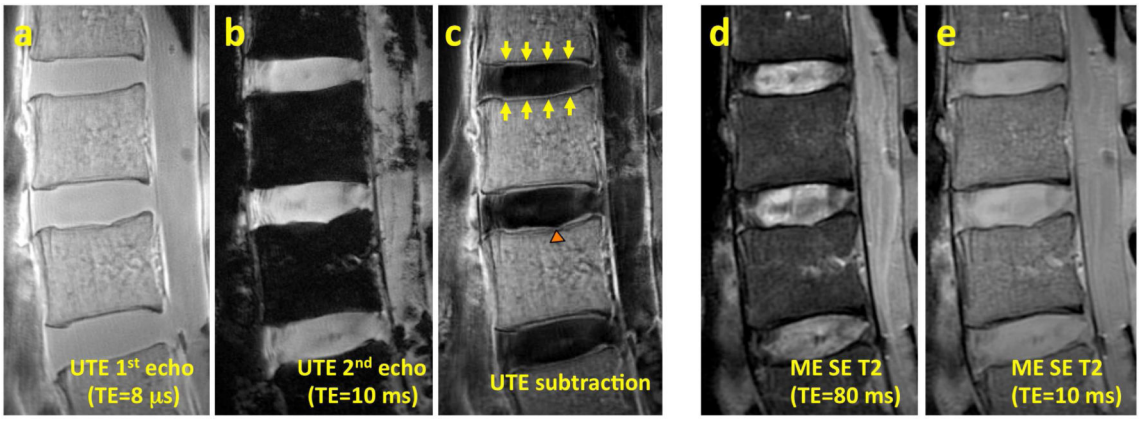

Figure 1.

Sagittal MR images of a lumbar spine with relatively normal vertebral endplates. (**a**) Ultrashort Echo Time (UTE) 1st echo and (**b**) 2nd echo images were digitally-subtracted to obtain (**c**) UTE subtraction MR image. This image shows normal cartilaginous endplates (CEP; arrows) are seen with continuous, linear and high signal intensity adjacent to hypointense vertebral endplates. A focal region of CEP thinning and absence of the signal intensity (arrowhead) can also be seen. In the corresponding (**d**) T2-weighted (obtained with multi-echo spin echo T2, ME SE T2, sequence at echo time, TE, of 80 ms) and (**e**) proton density-weighted (obtained with ME SE T2 sequence at TE of 10 ms) MR images, the region of CEP is difficult to distinguish from surrounding tissues, subtle abnormalities could not be discerned.

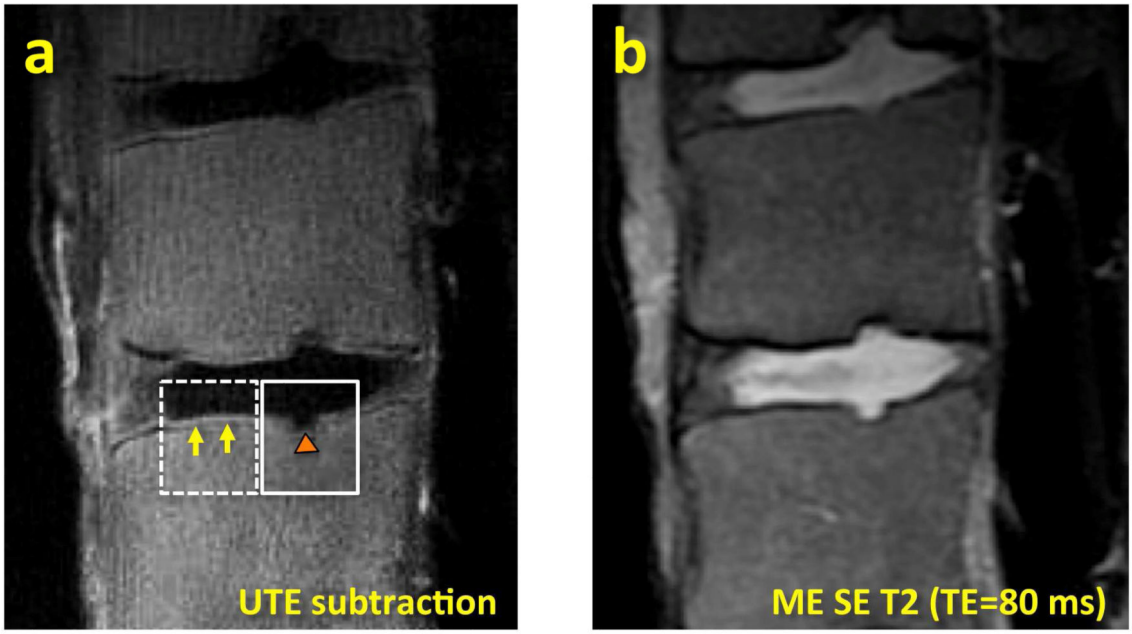

Figure 2.

Sagittal MR images of a lumbar spine with classic Schmorl nodes. (**a**) Ultrashort Echo Time (UTE) echo subtraction MR image shows a small classic Schmorl node (box) and an adjacent normal vertebral endplate (VEP; dotted box). Normal cartilaginous endplate (CEP; arrows) is seen over the normal VEP, while a focal absence of the signal intensity of the CEP (arrowhead) is seen over the Schmorl node. (**b**) In the corresponding T2-weighted MR image obtained with multi-echo spin echo T2 (ME SE T2) sequence at echo time (TE) of 80 ms, the abnormality of the CEP could not be discerned.

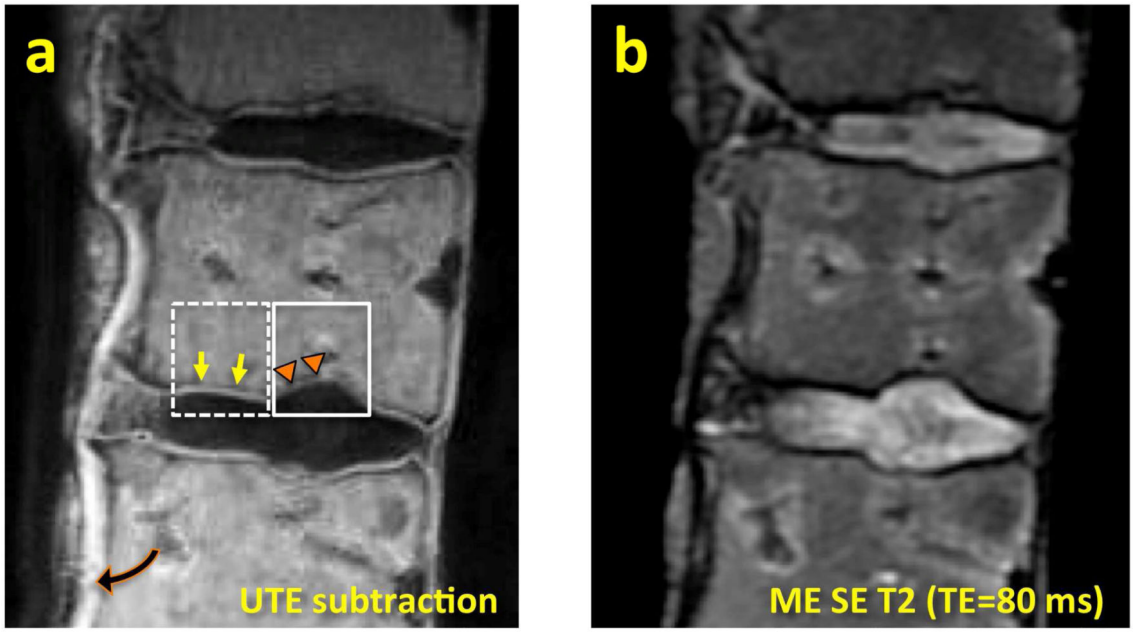

Figure 3.

Sagittal MR images of a lumbar spine with smooth indentations of the vertebral endplate (VEP). (**a**) Ultrashort Echo Time (UTE) echo subtraction MR image shows a smooth indentation of a superior VEP (box) and an adjacent normal VEP (dotted box). Normal cartilaginous endplate (CEP; arrows) is seen over the normal VEP, while a thin morphology of the signal intensity of the CEP (arrowhead) is seen over the VEP lesion. Thickening of the anterior longitudinal ligament (curved arrow) is seen. (**b**) In the corresponding T2-weighted MR image obtained with multi-echo spin echo T2 (ME SE T2) sequence at echo time (TE) of 80 ms, the abnormality of the CEP could not be discerned.

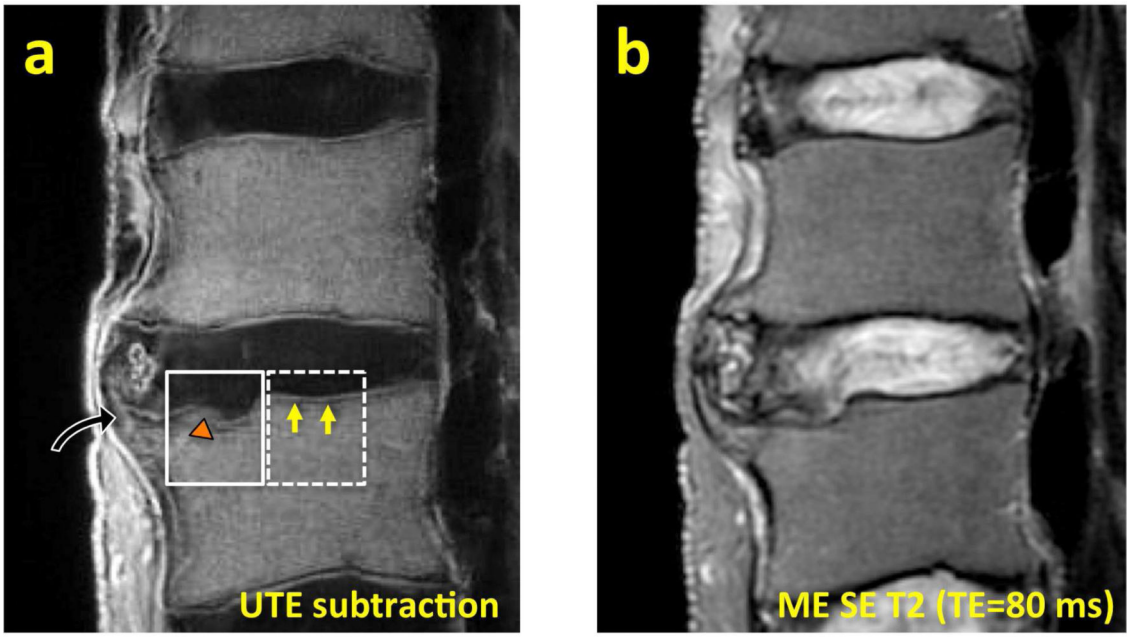

Figure 4.

Sagittal MR images of a lumbar spine with an irregular vertebral endplate (VEP) lesion. (**a**) Ultrashort Echo Time (UTE) echo subtraction MR image shows the VEP lesion (box) and an adjacent normal VEP (dotted box). Normal cartilaginous endplate (CEP; arrows) is seen over the normal VEP, while an irregular morphology of the signal intensity of the CEP (arrowhead) is seen over the VEP lesion. The presence of osteophytes (curved arrow) is seen. (**b**) In the corresponding T2-weighted MR image obtained with multi-echo spin echo T2 (ME SE T2) sequence at echo time (TE) of 80 ms, the abnormality of the CEP could not be discerned.

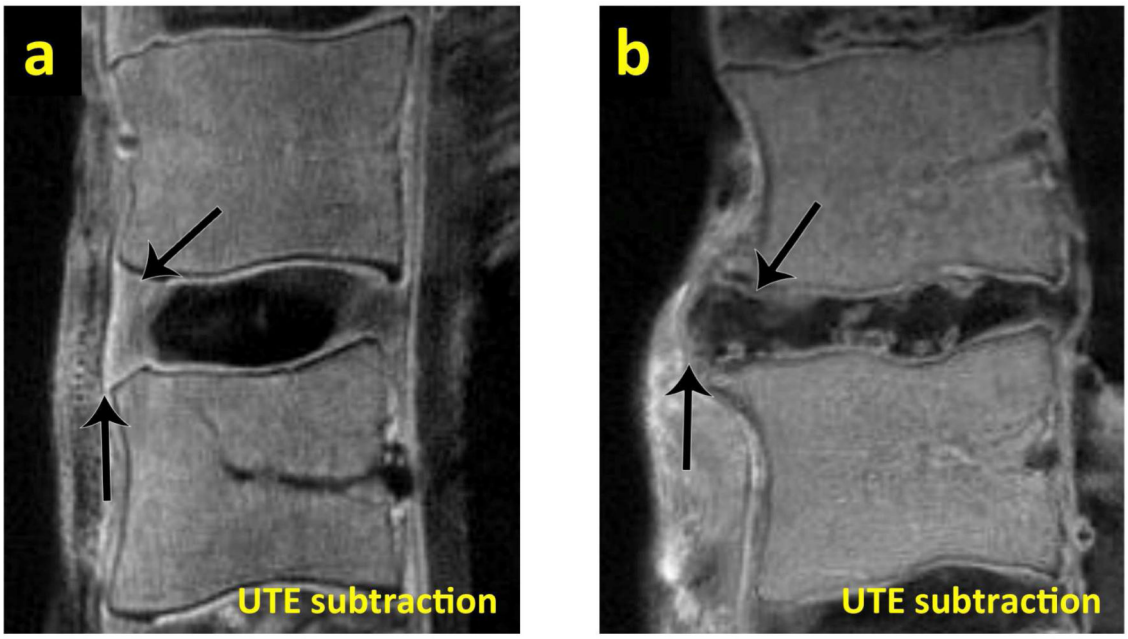

Figure 5.

Sagittal UTE echo subtraction MRI images of two lumbar spines. (**a**) **Normal disc:** Normal striated hyperintense appearance of the annulus fibrosus (diagonal arrow) and undulating curvilinear hyperintense appearance of the anterior longitudinal ligament (up arrow). (**b**) **Degenerated disc:** Globular signal alteration within the intervertebral disc with disruption of the normal striated fibers of the annulus fibrosus (diagonal arrow) and signal alteration of the buckled anterior longitudinal ligament (up arrow).

Table 1

MR scanning parameters.

Sequence	TR (ms)	TE (ms)	Flip Angle (degrees)	Slice (mm)	FOV (cm)	Phase × Frequency	Recon Matrix
UTE	500	0.008 and 10	45	3	16 to 20	455 × 512	512 × 512
ME SE T2	2000	10 to 80 (8 echoes)	90	3	16 to 20	320 × 256	512 × 512

Table 2

Different types of vertebral endplate (VEP) lesions including classic Schmorl nodes, smooth indentation, and irregular VEP, found at each spinal level.

VEP Lesion	T12/L1	L1/2	L2/3	L3/4	L4/5	All Levels
Classic Schmorl Node	4	5	4	3	0	16
Smooth	2	3	4	0	1	10
Irregular	7	10	5	5	2	29
All Types	**13**	**18**	**13**	**8**	**3**	**55**

Table 3

Morphology of CEP (including only those in consensus by two observers) found overlying normal VEP and VEP lesions.

		CEP Morphology (in consensus)					
		Normal	**Thin**	**Thick**	**Absent**	**Irregular**	**All CEPs**
Normal VEP		43	1	0	0	0	**44**
VEP Lesion Types	Classic Schmorl node	0	7	3	2	3	**15**
	Smooth	0	3	3	1	3	**10**
	Irregular	0	9	1	2	17	**29**
All VEPs		**43**	**20**	**7**	**5**	**23**	**98**